Local structure and electronic properties of an interstitial Ni^+ impurity in diamond

Yang Jinlong
*Chinese Center of Advanced Science and Technology (World Laboratory), P.O. Box 8730, Beijing 100080, People's Republic of China and Center for Fundamental Physics, University of Science and Technology of China, Hefei, Anhui 230026, People's Republic of China**

Zhang Manhong and Wang Kelin
Center for Fundamental Physics, University of Science and Technology of China, Hefei, Anhui 230026, People's Republic of China
(Received 25 June 1993; revised manuscript received 6 December 1993)

The local structure and electronic properties of an interstitial Ni^+ impurity in diamond are studied using the discrete-variational local-density-functional method with cluster models. The existence of a trigonal distortion about the impurity site is verified by the binding-energy calculation. The electronic-structure calculation shows that two optical absorption bands with zero-phonon lines at 1.40 and 3.1 eV and a broad absorption band centered near 1.4 eV, observed in synthetic diamond, are associated with the single interstitial Ni^+ impurity. The calculated results of the spin-orbit splitting of the ground state and the energy positions as well as polarization properties of the optical transitions are in good agreement with the experimental ones. An optical transition of about 2.5 eV is predicted, which reveals a different polarization property compared with the observed 2.51-eV absorption band and 2.56-eV luminescence band.

I. INTRODUCTION

Recent developments in the high-pressure synthesis of large diamond crystals have spawned an interest in the use of this material in electronic devices.[1] As is well known, diamond has many unusual properties such as its hardness and thermal conductivity. These properties make its use in devices subject to extreme conditions very attractive. Impurities and point defects, which usually spoil its unique physical properties, might sometimes create optical or electrical properties in practical applications.

Transition metals, particularly Ni, Co, Fe, and their alloys, are usually used as solvent catalysts when diamond crystals are synthesized. The growth conditions seem to be most favorable in incorporating transition-metal impurities into the lattice of diamond, but to date the only transition metal believed to enter diamond in the form of dispersed atoms is nickel.[2,3] In diamond, single Ni impurities can be found on a substitutional site with electronic configuration ($3d^7, S=\frac{3}{2}$) under T_d symmetry (hereafter, Ni_s^-), and on an interstitial site with electronic configuration ($3d^9, S=\frac{1}{2}$) under C_{3v} symmetry (hereafter, Ni_i^+). It is believed that they can also form complexes with themselves or other atoms in diamond.

Diamond crystals which have been synthesized in the presence of nickel give rise to optical-absorption bands with zero-phonon lines at 1.40, 1.883, 2.51, and 3.1 eV, a broad absorption band centered near 1.4 eV and luminescence bands with zero-phonon lines at 1.40 and 2.56 eV.[4-8] All of these systems are restricted to the {111} growth sectors of synthetic diamonds. The 1.40-eV system consists of a zero-phonon doublet which results from a slight splitting (2.9–3.3 meV) of the ground state. The higher-energy component of the doublet is observed only under a π polarization whereas the lower-energy component is seen in both σ and π polarization. The 2.56 system is made up of four closely spaced zero-phonon lines which arises most possibly from splittings of the excited state. It is strong when the 1.40-eV system is strong. The 3.1-eV system contains a series of absorption lines. It is strongest in diamonds containing a low nitrogen concentration. As for the other systems, it is found that the 1.4-eV system is also strongest in diamonds containing a low nitrogen concentration, whereas the 1.883- and 2.51-eV systems are strongest in diamonds with a high nitrogen concentration.

All the above systems are tentatively associated with nickel defects in diamond, but so far the forms of defects have not been known except for the 1.40-eV system. Recent experiments[9] have concluded that the 1.40-eV system arises from a single Ni_i^+ impurity and the transition is between a doubly degenerate orbital ground state (^2E), which is split by spin-orbital interaction, and a nondegenerate orbital excited state (^2A) with C_{3v} symmetry. Theoretically, Paslovsky and Lowther[10,11] have calculated the electronic structure of a single Ni_i^+ impurity under C_{3v} symmetry using a semiempirical complete neglect of differential overlap (CNDO) method. Two impurity levels e and a_1 are introduced into the host crystal gap due to the presence of the impurity in their calculation. The a_1 level is just above the valence-band edge (E_v), while the e level is at $E_v+2.33$ eV. They suggested that the transition between them correspond to the observed 1.40-eV system. They also estimated the ground-state splitting induced by the spin-orbital interaction to be 1.84 meV. All their results give a qualitative explanation for the 1.40-eV system, and a complete quantitative description, based on a first-principles study, is still required.

In this paper, a first-principles approach with cluster models is employed to study the local structure and electronic properties of a single Ni_i^+ impurity in diamond.

The cluster model and computational method are described in Sec. II. Our results and discussions are presented in Sec. III. Finally, conclusions are given in Sec. IV.

II. CLUSTER MODEL AND COMPUTATIONAL METHOD

Cluster models are adopted in this paper, which have been used successfully to study the impurity problems in semiconductors.[12–14] In cluster models, the perfect crystal is simulated by the cluster containing a certain number of the host atoms with an appropriate boundary condition (hereafter, perfect cluster), and the impurity-doped crystal is simulated by the so-called defect cluster, which can be obtained by suitable modifications of the perfect cluster. For diamond, we choose a cluster $C_4C_6C_{12}C_8$, which consists of successive shells of nearest-neighbor (NN) carbon atoms around an interstitial site, as our perfect cluster. For an interstitial Ni^+ in diamond, the corresponding defect cluster $NiC_4C_6C_{12}C_8$ is formed by placing a Ni^+ ion at the interstitial center of the perfect cluster.

In our calculations, two kinds of boundary conditions are added to clusters for different purposes. The first one is the free boundary condition, in which the problem of the saturation of the dangling bonds at the cluster surface is not considered. It is used to optimize the local structure of the impurity, where only the central Ni^+ ion and the four NN C atoms surrounding the impurity are allowed to relax. In such a kind of study, we are only interested in the difference of binding energies of clusters, which should not be changed greatly by the choice of boundary conditions when clusters are large.[15] We will further examine the accuracy of such an approximate approach in Sec. III A.

In order to calculate accurately the electronic structure of diamond with and without a single Ni_i^+ impurity, however, the problem left out above must be considered. To solve the problem, we add the second kind of boundary condition—the Watson sphere boundary condition[16,17]—to clusters. In this boundary condition, the rest of the crystal at the cluster boundary is simulated by first identifying V, the number of electrons in the cluster which corresponds to the valence states of the perfect crystal. In diamond, each C atom has four valence electrons and forms four C-C covalent bonds with its four nearest neighbors. According to the sp^3 hybridization, each C atom contributes one electron to each of C-C bonds, thus, V is the sum of the valence electrons of C atoms contributing to all the saturated C-C covalent bonds in the cluster. If N is the total number of valence electrons in the cluster, there will be $N-V$ electrons filling dangling bonds at its surface. These electrons are transferred to a sphere (Watson sphere) surrounding the cluster and are kept fixed throughout calculations. The perfect cluster $C_4C_6C_{12}C_8$ has $V=80$ and $N=120$, so we eliminate dangling bond effects by transferring $N-V=40$ electrons to the Watson sphere. For the defect cluster $NiC_4C_6C_{12}C_8$, we assume that it has the same crystalline environment as the perfect cluster. The Watson sphere radius is chosen as the average distance of the outermost shell of atoms in the cluster and the first shell of atoms outside the cluster to the center of the cluster, that is 6.684 a.u.

The binding energy and electronic structure of clusters are performed using the discrete-variational local-density-functional (DV-LDF) method. This method is a kind of molecular-orbital calculation method and its theoretical foundation is LDF theory. Since it has been described in detail elsewhere,[18–20] here we do not give a further description. In our calculations, the numerical atomic basic functions are chosen as the variational basis set, which are obtained from the self-consistent atomic LDF calculations. We choose 1*s*-2*p* for C and 1*s*-4*p* for Ni, and treat the low-energy orbitals as frozen cores. The exchange-correlation potential is taken to be of the von Barth-Hedin form,[21] with the parameters taken from Moruzzi, Janak, and Williams.[22]

III. RESULTS AND DISCUSSIONS

A. Local structure

Experiments[3,9] indicate a distortion at the single Ni_i^+ impurity site, lowering the point-group symmetry from tetrahedral (T_d) to trigonal (C_{3v}). To determine the local structure of the impurity, we calculate the binding energy of the $NiC_4C_6C_{12}C_8$ cluster as the impurity ion is moved off the perfect interstitial site in the $\langle 111 \rangle$ direction. Curve (a) in Fig. 1 is a plot of the cluster binding energy versus the off-center distortion, given in the $\langle 111 \rangle$ displacement from the perfect interstitial site. The minimum-energy atomic configuration for the cluster shows the impurity 0.2 a.u. away from its interstitial site along the $\langle \bar{1}\,\bar{1}\,\bar{1} \rangle$ direction (in our cluster, one of the NN C atoms is placed on the $\langle 111 \rangle$ axis). This result indicates the existence of a trigonal distortion about the impurity site, and is consistent with the experimental obser-

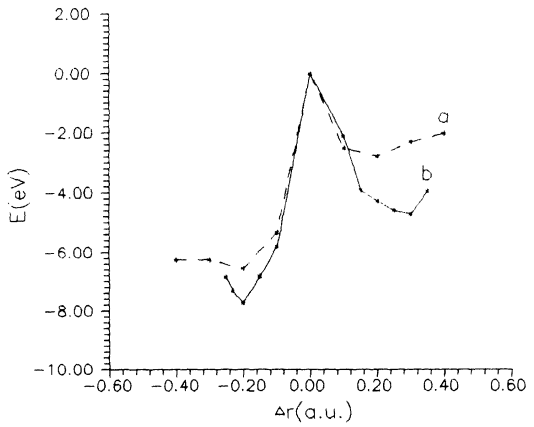

FIG. 1. Plots of the cluster binding energy versus the off-center distortion of the impurity, given in the $\langle 111 \rangle$ displacement from the perfect interstitial site. Curves (a) and (b) stand for the situations without and with relaxations of the four NN carbon atoms surrounding the impurity, respectively.

vation for the Ni_i^+ impurity.

In order to obtain a more accurate local structure for the electronic structure calculation, we further allow the four NN carbon atoms surrounding the impurity to relax trigonally at each displacement of the impurity, using the normalized distortion mode method.[23] Curve (b) in Fig. 1 shows the behavior of the cluster binding energy with this relaxation. At the equilibrium atomic configuration, we obtain the stable position of the Ni_i^+ impurity is still at 0.2 a.u. away from its interstitial site along the $\langle \bar{1}\,\bar{1}\,\bar{1} \rangle$ direction, while for the NN C atom on the $\langle 111 \rangle$ axis, the distance from the atom itself to the interstitial site is changed from 2.92 to 2.68 a.u.; for each of the other three NN C atoms, the length of the radius vector joining the atom itself to the interstitial site is changed from 2.92 to 2.99 a.u., and its angle with the $\langle 111 \rangle$ axis is changed from 70.53° to 72.62°.

Our result for the stable position of the Ni_i^+ impurity is in good agreement with that of Paslovsky and Lowther,[10,11] obtained by including the effects of the relaxation of the four NN carbon atoms. This agreement confirms that the free boundary condition is a good approximation for the present study. Certainly, we should point out that, without the relaxation of the four NN carbon atoms, Paslovsky and Lowther[10,11] found the impurity 0.08 a.u. away from the perfect interstitial site along the $\langle 111 \rangle$ direction, in contrast to our result. We think this discrepancy most possibly comes from the nature of CNDO method.

The optimization of the local structure of the impurity Ni_i^+ in the free boundary condition is only an approximate approach. The accuracy of this approach is examined by performing binding-energy calculations to determine the equilibrium positions of the first-shell atoms of the perfect cluster $C_4C_6C_{12}C_8$. We allow the first-shell atoms of the perfect cluster to relax symmetrically outward and toward from the interstitial center, holding the remaining atoms fixed at their ideal lattice positions. Figure 2 shows the curve of the binding energy versus the displacement of the first-shell atoms from the ideal lattice positions for the perfect cluster. One can find that the first-shell atoms hardly relax. This result indicates that the surface dangling bonds in the free boundary condition have a very small influence on the local geometry around the interstitial center. Thus, it is possible for us to determine the local structure of an interstitial Ni^+ impurity in diamond using the free boundary condition.

B. Electronic properties

With its local structure obtained above, we calculate the electronic structure of a single Ni_i^+ impurity in diamond, using the defect cluster $NiC_4C_6C_{12}C_8$ with C_{3v} distortion under the Watson sphere boundary condition. As comparison, we also calculate the electronic structure of the defect cluster $NiC_4C_6C_{12}C_8$ without C_{3v} distortion and the corresponding perfect cluster $C_4C_6C_{12}C_8$.

For the perfect cluster, the lowest occupied molecular orbital (LOMO), the highest occupied molecular orbital (HOMO) and the lowest unoccupied molecular orbital (LUMO) are $1a_1$, $3t_1$, and $5a_1$, respectively. The energy difference between HOMO and LUMO is the so-called crystal gap E_g in cluster models, which is 5.2 eV. The energy difference between HOMO and LOMO is defined as the valence-band (VB) width E_{vb}, which is 19.8 eV. These two values are in good agreement with the experimental ones[24] $E_g = 5.4$ eV and $E_{vb} = 21.0$ eV for the bulk crystal.

Figure 3 presents the valence-band part of the densities of states (DOS) for the perfect cluster, which is obtained by a Lorentzian extension. For comparison, the valence-band part of the DOS calculated by Painter, Ellis, and Lubinsky[25] is also included. From Fig. 3, one can see that our DOS is in good agreement with that of Painter, Ellis, and Lubinsky. All the above results obviously suggest that the electronic environment in this cluster is already reasonably bulklike, and the Watson sphere boundary condition can be used to study the impurity problems

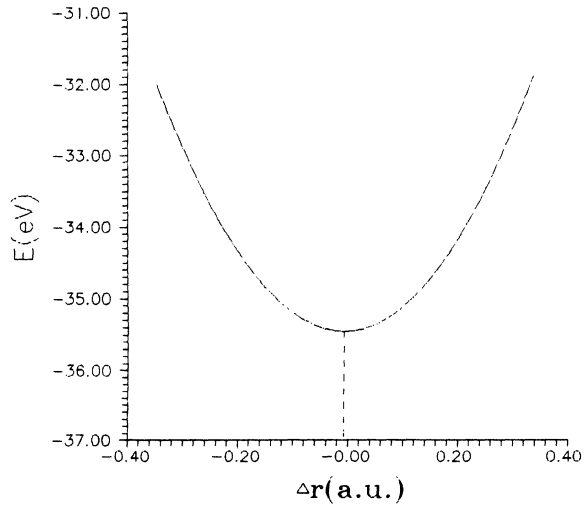

FIG. 2. The cluster binding energy versus the displacement of the first-shell atoms of the perfect cluster $C_4C_6C_{12}C_8$. The $-ve$ displacement is towards the center.

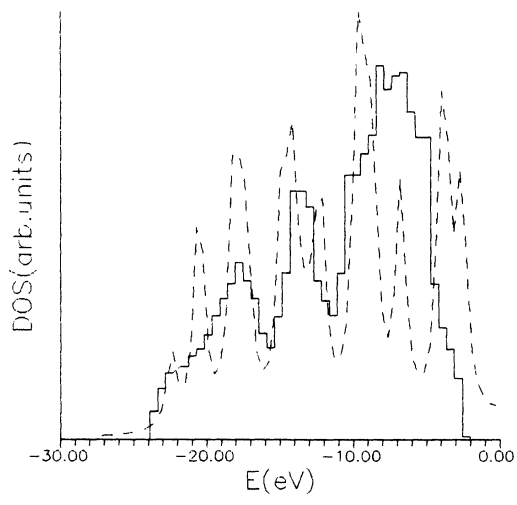

FIG. 3. The valence-band part of DOS of the perfect cluster $C_4C_6C_{12}C_8$ (dashed line) and the valence-band part of DOS of diamond calculated by Painter, Ellis, and Lubinsky (solid line).

in diamond.

In the defect cluster without C_{3v} distortion, the Ni $3d$ levels are split into states of e and t_2 symmetry by the tetrahedral field of the neighboring host atoms. The e and t_2 components hybridize with ligand states of e and t_2 symmetry, respectively, leading to $3e$, $4e$, $7t_2$, and $8t_2$ levels with substantial d-like character. The valence-band parts of DOS of the perfect cluster, the defect cluster and the Ni $3d$ partial density of states (PDOS) in the defect cluster under T_d symmetry are shown in Fig. 4. The percent Ni $3d$ character and energy positions of nickel-related levels are given in Fig. 5(a). From these two figures, one can see that only the $4e$ level appears in the vicinity of the host band gap. It is occupied by three electrons, giving a doubly degenerate orbital ground state (^2E). The transition energies between the gap state ($4e$) and the impurity-related states ($3e$, $7t_2$, and $8t_2$) in the valence band are 1.33, 2.51, and 3.06 eV, respectively. They are so close to the values of 1.40 or 1.4, 2.51, or 2.56, and 3.1 eV that one may link the transitions with the observed 1.40-eV system or 1.4-eV system, 2.51-eV system or 2.56-eV system, and 3.1-eV system, respectively. Below, we analyze their properties and give definite assignments for them, using the electronic structure results of the defect cluster with C_{3v} distortion.

Lowering in point symmetry of the tetrahedral environment from that of T_d to C_{3v} produces splittings of the t_1 and t_2 degenerate states into trigonal states (a_2,e) and (a_1,e), respectively. As a result, the impurity-related levels in the defect cluster with C_{3v} distortion become $11a_1$, $12a_1$, $11e$, $12e$, $13e$, and $15e$ levels. The $15e$ level falls in the band gap. Figure 5(b) gives their percent Ni $3d$ character and energy positions.

First, we consider the transition between $15e$ and $12a_1$, whose transition energy is 1.46 eV. If we use many-electron configurations to describe transitions, this transition is between a doubly degenerate orbital ground state

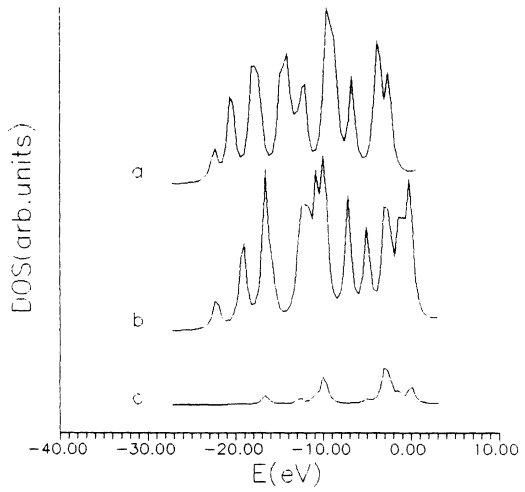

FIG. 4. The valence-band parts of DOS of the perfect cluster $C_4C_6C_{12}C_8$ (a), the defect cluster $NiC_4C_6C_{12}C_8$ (b), and the Ni $3d$ PDOS in the defect cluster (c) under T_d symmetry.

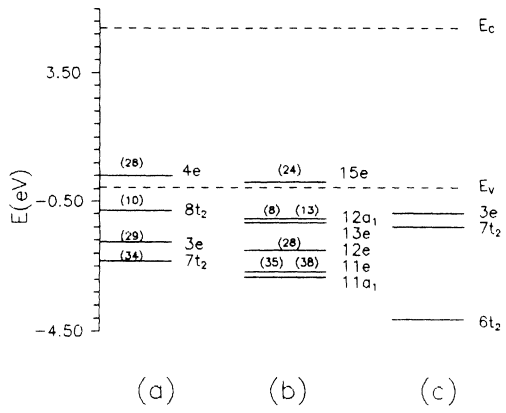

FIG. 5. The percent Ni $3d$ character and energy positions of the impurity-related levels in the defect cluster: (a) without C_{3v} distortion and (b) with C_{3v} distortion. As a reference, the part levels of the perfect cluster are also presented (c).

(^2E) and a nondegenerate orbital excited state (^2A), which agrees with that deduced from the observed 1.40-eV system.[9] The relative intensities of the dipole-transition in the $\langle 1\bar{1}0\rangle$, $\langle 11\bar{2}\rangle$, and $\langle 111\rangle$ directions are 5.58, 5.58, and 0.0, respectively (Table I), showing that this transition is restricted to the $\{111\}$ growth sectors, again in good agreement with the experimental result[7] for the 1.40-eV system. Hence, we assign this transition to the observed 1.40-eV system. To further explain the double of the 1.40-eV system and their different polarization properties, we need to consider the spin-orbit interaction. With the spin-orbit coupling, the ^2E ground state ($15e^3$) is written as a product of a spatial part and a spin part. The spatial part transforms as the e irreducible representation of C_{3v} point group and is obtained from our electronic structure calculation, while the spin part is simply denoted as $|\alpha\rangle$ and $|\beta\rangle$. Using the effective spin-orbit Hamiltonian $H_{so}=\xi(L\cdot S)$ with a fictitious effective angular orbital momentum $L=1$ and a spin of $\frac{1}{2}$,[10] the eigenvalues and eigenfunctions of the spin-orbit secular matrix are

$$
\begin{aligned}
&+\tfrac{1}{2}\lambda,\Gamma_5:\\
&\quad|\psi_1^g\rangle=\sqrt{1/2}(|e_x\alpha\rangle+i|e_y\alpha\rangle)\,,\\
&\quad|\psi_2^g\rangle=\sqrt{1/2}(|e_x\beta\rangle-ie_y\beta\rangle)\,,
\end{aligned}
\tag{1}
$$

TABLE I. Relative dipole-transition intensities of the impurity related optical transitions under C_{3v} symmetry. Here x, y, and z axes are along $\langle 1\bar{1}0\rangle$, $\langle 11\bar{2}\rangle$, and $\langle 111\rangle$ directions of diamond.

Transitions	x	y	z
$15e\leftrightarrow 12a_1$	5.58	5.58	0.0
$15e\leftrightarrow 13e$	2.34	2.34	1.56
$15e\leftrightarrow 12e$	0.0	0.0	1.84
$15e\leftrightarrow 11e$	0.36	0.36	0.36
$15e\leftrightarrow 11a_1$	0.72	0.72	0.0

$-\frac{1}{2}\lambda, \Gamma_4$:

$$|\psi_3^g\rangle = \sqrt{1/2}(|e_x\alpha\rangle - i|e_y\alpha\rangle) ,$$
$$|\psi_4^g\rangle = \sqrt{1/2}(|e_x\beta\rangle + i|e_y\beta\rangle) , \quad (2)$$

where Γ_5 and Γ_4 representations of C_{3v}^* double-point group. They are two Kramers doublets and separated in energy by λ. Using the formula in Ref. 11 and the data from our electronic-structure calculation, we obtain $\lambda = 3.2$ meV, which compares well with the observed splitting of 2.9–3.3 meV.[5]

In the same way, we can write down the eigenfunctions of the ^2A excited state ($12a_1^1 15e^4$) as $|a_1\alpha\rangle$ and $|a_1\beta\rangle$, which transforms as the Γ_4 representation of C_{3v}^* double-point group. The spin-orbit interaction also splits the excited state ($13e^3 15e^4$), the eigenfunctions of the spin-orbit secular matrix are similar to the right hands of Eqs. (1) and (2). Since the energy difference between these two excited states is small, the excited states ^2A and ^2E will be mixed within the Γ_4 representation of C_{3v}^* double-point group. Thus, the final eigenfunctions of the ^2A excited state can be expressed as Γ_4:

$$|\psi_1^e\rangle = -a|a_1\beta\rangle + b\sqrt{1/2}(|e_x'\alpha\rangle - i|e_y'\alpha\rangle) ,$$
$$|\psi_2^e\rangle = +a|a_1\alpha\rangle + b\sqrt{1/2}(|e_x'\beta\rangle + i|e_y'\beta\rangle) , \quad (3)$$

where coefficients a and b depend on the energy splittings induced by the trigonal distortion and the spin-orbit interaction.

We denote transitions $|\psi_1^g\rangle, |\psi_2^g\rangle \leftrightarrow |\psi_1^e\rangle, |\psi_2^e\rangle$ and $|\psi_3^g\rangle, |\psi_4^g\rangle \leftrightarrow |\psi_1^e\rangle, |\psi_2^e\rangle$ as the μ and ν lines, respectively. The intensities of μ and ν, excited by light linearly polarized parallel and perpendicular to the $\langle 111\rangle$ direction, are calculated as

$$I_{\mu\perp} \cong 2.79a^2 + 1.17b^2 ,$$
$$I_{\mu\parallel} \cong 0.0 , \quad (4)$$

$$I_{\nu\perp} \cong 2.79a^2 + 1.17b^2 ,$$
$$I_{\nu\parallel} \cong 0.78b^2 . \quad (5)$$

From Eqs. (4) and (5), one may see that the higher component μ only has π polarization while the lower one ν has different π to σ polarization with different a and b. These are the same as the polarization properties of the experimental 1.40-eV zero-phonon doublet.[8]

Second, we consider the transition from $13e$ to $15e$, whose transition energy is 1.50 eV. Since the $13e$ has only 13% Ni $3d$ character and mainly consists of the first NN carbon atoms orbitals, the strong dynamic $e \otimes E$ coupling makes this transition very diffuse and produces a broad absorption band with maximum at 1.50 eV. This effect can be understood by noticing that there is a bulk-like level ($7t_2$) at the energy position of the $13e$ in the perfect cluster [Fig. 5(c)]. We suggest that this transition correspond to the observed 1.4-eV system.

Thirdly, we consider transitions from ($11a_2, 11e$) to $15e$, whose transition energies are 3.05 and 3.28 eV, respectively. They are assigned to the observed 3.1-eV system. From Table I one can see that for the transition from $11e$ to $15e$, the relative intensities in $\langle 1\bar{1}0\rangle$, $\langle 11\bar{2}\rangle$, and $\langle 111\rangle$ directions are 0.36, 0.36, and 0.36, respectively; for the transition from $11a_1$ to $15e$, the relative intensities are 0.72, 0.72, and 0.0, respectively. So for the transitions from ($11a_1, 11e$) to $15e$, the allowed dipole transitions are mainly in the $\langle 1\bar{1}0\rangle$ and $\langle 11\bar{2}\rangle$ directions, showing that these transitions are restricted to the $\{111\}$ growth sectors, in good agreement with the experimental result[7] for the 3.10-eV system. If we consider the spin-orbital interaction in these transitions, there will be six zero-phonon lines, explaining satisfactorily the composition of the 3.1-eV system.[7]

Our suggestion that the 1.4- and 3.1-eV systems arise from a single Ni_i^+ impurity can account for the experimental relation[7] between their relative intensities and the nitrogen concentration in the diamond. The intensities of these systems decrease when increasing amounts of nitrogen are present in the diamond. As nitrogen is usually a donor in diamond, the implication of such an observation is that the donor electron is being transferred to the Ni_i^+ and, in doing so, lowering the concentration of optically active Ni_i^+ ions.

Finally, we discuss the transition between $12e$ and $15e$, whose transition energy is 2.50 eV. The relative intensities of the transition in $\langle 1\bar{1}0\rangle$, $\langle 11\bar{2}\rangle$, and $\langle 111\rangle$ directions are 0.0, 0.0, and 1.84, respectively (Table I), its allowed dipole transition is only in the $\langle 111\rangle$ direction, indicating that this transition is restricted to the non-$\{111\}$ growth sectors. This result contradicts obviously the experimental observations[7] for the 2.51- and 2.56-eV systems. With this transition, moreover, we could not explain the experimental facts as follows: (1) the 2.51-eV system is strongest in diamonds containing a high nitrogen concentration,[7] and (2) the temperature dependence of the 2.56-eV system indicates the center has a singlet ground state.[5] Hence, this transition corresponds neither to the 2.51-eV system nor the 2.56-eV system. We think this transition is a new optical transition. It is worth noticing that the energy position and polarization property of this transition are similar to those of the observed $H3$ system,[7] which is a luminescence band with a zero-phonon line at 2.463 eV arising from the N-V-N defect in diamonds. This may be one of the reasons that this transition has not been observed so far.

It should be pointed out that in our study, we do not consider charge compensators of the Ni_i^+ impurity. Isoya, Kanda, and Uchida have measured[2] the temperature dependence of the electron paramagnetic resonance spectrum of the impurity, they found that at 4 K, the line shape is asymmetric and depends on the orientation of the crystal with respect to the magnetic field; between 25 and 77 K, the line shape is independent of the orientation of the crystal. According to this, they concluded that the charge-compensating ions (defects) are located a large distance apart. So not considering charge compensators does not cause a large error to the electronic structure of the impurity.

IV. CONCLUSIONS

In this paper, we have studied the local structure and electronic properties of an interstitial Ni^+ impurity in di-

amond using the DV-LDF method with cluster models. The local structure of the impurity is determined by the binding-energy calculation, which verifies the existence of a trigonal distortion about the impurity site. The electronic-structure calculation shows that two optical-absorption bands with zero-phonon lines at 1.40 and 3.1 eV and a broad absorption band centered near 1.4 eV, observed in synthetic diamond, are associated with the single interstitial Ni^+ impurity. The spin-orbit splitting of the ground state and the energy positions as well as polarization properties of the optical transitions are calculated and found to be in good agreement with the experimental ones. An optical transition of about 2.5 eV is predicted, which reveals a different polarization property compared with the observed 2.51-eV absorption band and 2.56-eV luminescence band.

ACKNOWLEDGMENTS

This research was supported by the National Natural Science Foundation of China and by the Youth Natural Science Foundation of USTC.

---

*Mailing address.

[1]J. C. Angus and C. C. Hayman, Science **241**, 913 (1988).
[2]J. Isoya, H. Kanda, and Y. Uchida, Phys. Rev. B **42**, 9843 (1990).
[3]J. Isoya, H. Kanda, J. R. Norris, J. Tang, and M. K. Bowman, Phys. Rev. B **41**, 3905 (1990).
[4]A. T. Collins and P. M. Spear, J. Phys. D **15**, L183 (1982).
[5]A. T. Collins and P. M. Spear, J. Phys. C **16**, 963 (1983).
[6]G. Davies, A. J. Neves, and M. H. Nazare, Europhys. Lett. **9**, 47 (1989).
[7]A. T. Collins, H. Kanda, and B. C. Burns, Philos. Mag. B **61**, 797 (1990).
[8]A. T. Collins, J. Phys. Condens. Matter **1**, 439 (1989).
[9]M. H. Nazare and A. J. Neves, Phys. Rev. B **43**, 14 196 (1991).
[10]L. Paslovsky and J. E. Lowther, J. Phys. Condens. Matter **4**, 775 (1992).
[11]L. Paslovsky and J. E. Lowther, Solid State Commun. **80**, 542 (1992).
[12]R. Satio and T. Kiraura, Phys. Rev. B **46**, 1423 (1992).
[13]P. K. Khowash, Phys. Rev. B **43**, 9931 (1991).
[14]N. Gemma, J. Phys. C **17**, 2333 (1984).
[15]Yang Jinlong, Wang Kelin, and F. Casula, in *Computational Methods in Materials Science,* edited by J. E. Mark, M. E. Glicksman, and S. P. Marsh, MRS Symposia Proceedings No. 278 (Materials Research Society, Pittsburgh, 1992), p. 121.
[16]A. Fazzio, J. R. Leite, and M. L. De Siqueira, J. Phys. C **12**, 513 (1979).
[17]A. Fazzio and J. R. Leite, Phys. Rev. B **21**, 4710 (1980).
[18]G. S. Painter and D. E. Ellis, Phys. Rev. B **1**, 4747 (1970).
[19]A. Rosen, D. E. Ellis, H. Adachi, and F. W. Averill, J. Chem. Phys. **65**, 3629 (1976).
[20]B. Delley, D. E. Ellis, A. J. Freeman, E. J. Baerends, and D. Post, Phys. Rev. B **27**, 2132 (1983).
[21]U. von Barth and L. Hedin, J. Phys. C **5**, 1629 (1972).
[22]V. L. Moruzzi, J. F. Janak, and A. R. Williams, *Calculated Electronic Properties of Metals* (Plenum, New York, 1978).
[23]G. D. Watkins and R. P. Messmer, Phys. Rev. B **7**, 2568 (1973).
[24]T. Gora, R. Staley, J. D. Rimstidt, and J. Sharma, Phys. Rev. B **5**, 2309 (1972).
[25]G. S. Painter, D. E. Ellis, and A. R. Lubinsky, Phys. Rev. B **4**, 3610 (1971).